Transport, thermoelectric, and thermal expansion investigations of the cage structure compound $CeOs_2Al_{10}$

C. S. Lue and H. F. Liu
Department of Physics, National Cheng Kung University, Tainan 70101, Taiwan

B. D. Ingale, J. N. Li, and Y. K. Kuo*
Department of Physics, National Dong Hwa University, Hualien 97401, Taiwan

(Received 9 November 2011; revised manuscript received 16 April 2012; published 15 June 2012)

In order to shed light on the electrical and thermal properties of the cage-type $CeOs_2Al_{10}$, we investigate this material by measuring electrical resistivity, Seebeck coefficient, thermal conductivity, specific heat, and thermal expansion. The phase transition $T_0 \sim 28$ K for $CeOs_2Al_{10}$ has been characterized by marked features in all measured physical quantities. Above T_o, the electrical resistivity and Seebeck coefficient can be well described by a two-band model with reliable physical parameters. Furthermore, the extracted magnitude of the quasielastic linewidth $q_f \sim 30.2$ K is found to be consistent with that observed in the neutron scattering experiment. These results are compared to its isostructural compound $CeRu_2Al_{10}$.

DOI: 10.1103/PhysRevB.85.245116 PACS number(s): 72.15.Qm, 72.15.Jf, 65.40.gh

I. INTRODUCTION

Over the past few decades substantial progress has been made in the understanding of magnetic,[1–3] thermal,[4–7] and electrical[3–8] properties on Ce-based intermetallic systems. However, these systems are still the subject of intense research mainly because of a variety of different novel magnetic/nonmagnetic ground states, such as heavy-fermion (HF), antiferromagnetic (AF) nature, mixed-valence (MV) and intermediate-valence (IV) states, spin or charge gap formation, charge-density wave (CDW), and spin-density wave (SDW), etc., due to the competition between Kondo and Ruderman-Kittel-Kasuya-Yoshida (RKKY) interactions.[5–7] It is well known that the hybridization between the localized $4f$ and conduction electrons (c-f hybridization) would lead to the formation of a hybridized gap in these Kondo semiconductors. Recently, the Ce-based aluminides CeM_2Al_{10} (M = Fe, Ru, and Os) have drawn considerable attention because of their wide variety of strongly correlated electronic properties.[9–13] Kondo insulator behavior for $CeFe_2Al_{10}$ and intriguing phase transitions at $T_0 \sim 27$ K for $CeRu_2Al_{10}$ and transition temperature $T_0 \sim 28$ K for $CeOs_2Al_{10}$ have been reported. These compounds crystallize in the orthorhombic $YbFe_2Al_{10}$-type structure,[14,15] where each rare-earth Ce atom is encapsulated in a polyhedron cage formed by 16 Al and four M atoms. In spite of having a comparable T_0, the resistivity of the $CeRu_2Al_{10}$ system exhibits "metallic" behavior[4] below the phase transition down to 2 K, while the $CeOs_2Al_{10}$ system displays a thermal-activation-type temperature dependence[16] below 15 K, and that of isostructural $CeFe_2Al_{10}$ is a typical Kondo semiconductor, even at very low temperatures.[17] A fundamental issue in the electronic deposition of the two systems has been established by recent high-pressure studies.[5] When the pressure is applied to $CeRu_2Al_{10}$, T_0 disappears suddenly between 3 and 4 GPa and it turns into a Kondo semiconductor, and then into a metal. Interestingly, the electrical resistivity of $CeRu_2Al_{10}$ under hydrostatic pressure of 1.75 GPa is comparable to the overall behavior for $CeOs_2Al_{10}$ without applying pressure.[5] This indicates that the application of external pressure is effectively tuning the $4f$ band with respect to Fermi energy (ε_F) in a narrow-band system. These observations suggest that the corresponding ε_F for $CeRu_2Al_{10}$ and $CeOs_2Al_{10}$ locates at opposite sides of the center of gravity of the $4f$ band.

Very recently, it has been confirmed that the phase transition occurring at T_0, whose origin has been a subject of considerable debate, is unambiguously magnetic due to ordering of the Ce sublattice.[16] The long-range antiferromagnetic (AFM) ordering with small magnetic moments in both $CeRu_2Al_{10}$ and $CeOs_2Al_{10}$ systems has been observed by muon spin relaxation (μSR) and neutron scattering experiments.[18,19] Its consistency with the macroscopic properties and the origin of long-range order in $CeRu_2Al_{10}$ have been investigated by Kondo *et al.*[20] with a high-field magnetization study (up to ~55 T) and the authors claimed that the AFM order in $CeRu_2Al_{10}$ is rather complicated. The magnetization curves for $H \| a$ and c axes behave as if the magnetic anisotropy in the AFM ordered phase is small, although there exists a large magnetic anisotropy in the paramagnetic phase, which favors the easy axis along the a axis. On the other hand, Khalyavin *et al.*[18] have reported that the AF magnetic moment is parallel to the c axis. These results indicate that the origin of T_0 is still an open question. However, a recent report of the crystalline electric field (CEF) effects by Hanzawa *et al.* elucidated the origin of such a high transition temperature and the extremely low value of ordered moments.[21] The details of CEF effects on Ce in CeM_2Al_{10} (M = Ru and Os) should play important roles for the local $4f$ electronic structure. Also, the on-site $4f$-$5d$ mixing contributes to the RKKY interaction that is responsible for the high transition temperature.[21] Other microscopic studies by inelastic neutron scattering (INS) measurements revealed a clear signature of excitation near 8 meV in the case of $CeRu_2Al_{10}$ (Ref. 22), while that of 11 meV for $CeOs_2Al_{10}$ (Ref. 18) due to the opening of an energy gap in the spin excitation spectrum. From the temperature-dependent polarized optical conductivity spectra below T_0, the change in the electronic structure revealed the Kondo semiconducting characteristic with an energy gap of about 10 meV along

the a and c axes for $CeOs_2Al_{10}$. In contrast, along the b axis, the energy gap opens at a higher temperature (~39 K) than T_0, presumably due to the formation of CDW.[23] Such charge instability associated with structural distortion was also observed by electron diffraction.[16] This indicates that the strong anisotropic Kondo effect in $CeOs_2Al_{10}$ is relevant to the anomalous magnetic phase transition below T_0. A nuclear magnetic resonance (NMR) investigation revealed an energy gap of about 120 K with residual density of states (DOS) at the Fermi level of $CeOs_2Al_{10}$, providing microscopic evidence for the presence of a pseudogap with finite charge carriers near the Fermi surfaces.[24] Furthermore, the recent optical conductivity measurement elucidated the intrinsic information of structural and AFM characteristics for $CeOs_2Al_{10}$.[23]

Along with the microscopic studies, the physical properties such as magnetic susceptibility (χ) and heat capacity (C_P) show clear thermally activated behavior below T_0.[5] These observations indicated that the phase transition may be accounted for by the formation of an energy gap over a portion of the Fermi surfaces.[1,5,16,17] While many efforts have been devoted to elucidating the nature of the phase transition, there has been little work associated with the state above the transition, essential to interpret the transport and thermoelectric characteristics. In this investigation, we performed transport, thermoelectric, and thermal expansion experiments to shed light on the fundamental physical properties of $CeOs_2Al_{10}$. We also found that the employment of a two-band model[7] to analyze the electrical resistivity (ρ) and Seebeck coefficient (S) data gives a good agreement with experimental observations above T_0. In spite of a relatively small quasielastic linewidth for $CeOs_2Al_{10}$ as compared to its isostructural compound $CeRu_2Al_{10}$, strong similarity was identified for these characteristics of both compounds.

II. EXPERIMENT AND DISCUSSION

Polycrystalline compound $CeOs_2Al_{10}$ was prepared by an ordinary arc-melting technique. Briefly, the mixture of 99.9% Ce, 99.99% Os, and 99.99% Al elemental metals with the stoichiometric ratio was placed in a water-cooled copper hearth and then melted several times in an argon flow arc melter. The weight loss during melting is less than 0.5%. To promote homogeneity, the as-cast sample was annealed in a vacuum-sealed quartz tube at 800 °C for seven days, followed by furnace cooling. A room-temperature x-ray diffraction taken with Cu $K\alpha$ radiation on the powder specimen was identified within the expected $YbFe_2Al_{10}$-type structure (space group $Cmcm$) with no noticeable impurity phase, as displayed in Fig. 1.

A. Electrical resistivity

Electrical resistivity data were obtained using a standard four-point probe method. The observed temperature dependence of $\rho(T)$ for $CeOs_2Al_{10}$ is displayed in Fig. 2. Upon reducing temperature, ρ increases monotonically and rises abruptly at $T_0 \sim 28$ K. It establishes a small upturn kink at $T_P \sim 18$ K and then continues to rise with further cooling. Thermally activated behavior mimicking semiconducting transport and a large magnitude of $\rho(T) \sim 4.77$ mΩ cm at

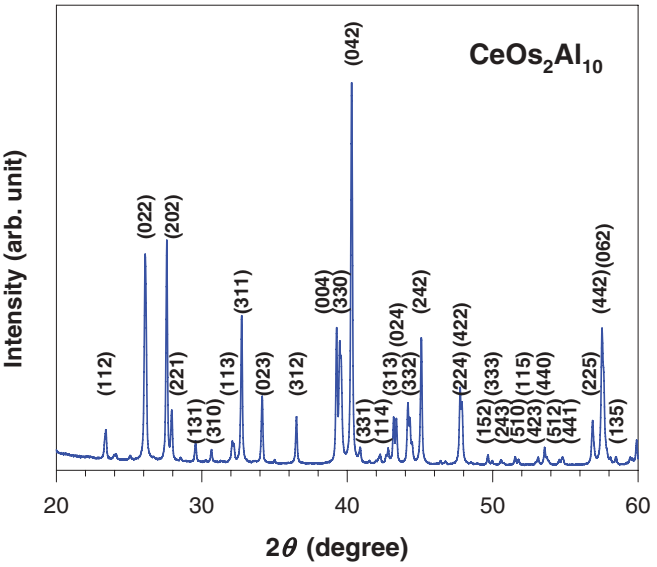

FIG. 1. (Color online) X-ray diffraction pattern for $CeOs_2Al_{10}$. The diffraction peaks were indexed according to the expected $Cmcm$ phase.

300 K are qualitatively similar to those of the hybridized f-electron systems such as $Ce(Cu_{0.97}Ni_{0.07})Si_2$ and URu_2Si_2.[3,7] An energy gap $\Delta_\rho = 44$ K is estimated by fitting $\rho(T)$ to $\exp(\Delta_\rho/2T)$ between 30 and 100 K, as shown in the inset of Fig. 2. This value is quite consistent with reported results.[5]

We further analyzed the electrical resistivity data above T_0 by using a two-band model where the dominant contribution to $\rho(T)$ arises from the scattering of electrons within a broad

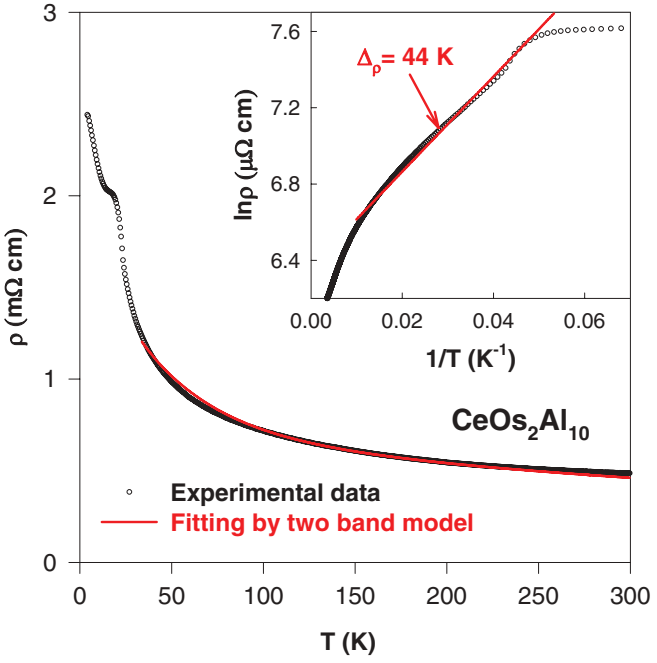

FIG. 2. (Color online) Electrical resistivity vs temperature for $CeOs_2Al_{10}$. The solid line is the fit to the measured data based on Eq. (1). Inset: a plot of ln ρ vs $1/T$, showing a linear portion between 30 and 100 K, revealing an energy gap of 44 K.

conduction band and a narrow Lorentzian-shaped $4f$ band.[25] The electronic DOS of the $4f$ band is expressed as $N(\varepsilon_F) = W/(W^2 + P^2)$, where W and P represent the width and the position of the narrow f-electron band, respectively. The position of the narrow f band is given by $P = (\varepsilon_F - E_f)/k_B$, where E_f is the energy corresponding to the center of gravity of the $4f$ peak in the DOS. It is important to note that the parameters W and P are temperature-dependent quantities that are crucial in interpreting the low-temperature thermoelectric properties (negative minimum in Seebeck coefficient) of Kondo systems.[7] Thus, the total resistivity in the absence of any anomalies due to structural or electronic phase transitions is given by

$$\rho = \rho_0 + cT + D\frac{W}{W^2 + P^2}, \tag{1}$$

with $W = q_f \exp(-q_f/T)$ and $P = A + B \exp(-m/T)$. Here A, B, and m are constants for a given compound. The parameter q_f is the fluctuation temperature, providing a measure of the quasielastic linewidth governing the Abrikosov-Suhl resonance that arises from the hybridization between the narrow $4f$ band and the surrounding broad conduction bands. Constants ρ_0, c, and D in Eq. (1) represent the temperature-independent residual resistivity, nonmagnetic phonon contribution, and the overlapping strength of the $4f$ band, respectively. In this model,[7] W is proportional to the DOS in the peak that would effectively take part in the scattering process at $N(\varepsilon_F)$. Thus, in the high-temperature limit, $W \approx q_f$ represents almost all the density of states in the narrow f band are effective in the scattering. Whereas, in the low-temperature limit, $W \ll q_f$ implies that only a tiny fraction of states contribute to the scattering process.

Figure 2 shows the nonlinear least-square fit to the experimental $\rho(T)$ data with respect to Eq. (1). It is evident that the two-band model describes the resistivity data quite satisfactorily over a wide temperature range from T_0 up to 300 K, compared to the simple-activation-type behavior which is merely agreeable from 30 to 100 K (inset in Fig. 2). It should be noted that only ρ_0, D, and q_f are free fitting parameters in the present analysis, while the values of A, B, and m are obtained from the analysis of the Seebeck coefficient $S(T)$ within the framework of this model as discussed in the following section. The magnitude of c is extracted from the slope of the ρ versus T plot within the temperature interval 250 K $< T <$ 300 K. We are thus able to determine the quasielastic linewidth $q_f = 30.2$ K, which is self-consistent with both $\rho(T)$ and $S(T)$ data. These physical parameters were tabulated in Table I.

Near T_0, the experimental $\rho(T)$ data deviate from the fit as the proposed model is not valid in the vicinity of the phase transition. Below T_0, the sudden increase in $\rho(T)$ is associated with the occurrence of a phase transition that opens a gap over a portion of Fermi surfaces. The feature may originate from charge instability or CDW formation due to structural distortion. It is worthwhile mentioning that the observed sharp rise below 20 K has also been found in the isostructural $CeFe_2Al_{10}$.[17] It is noted that there is a sharp rise in $\rho(T)$ for all CeM_2Al_{10} (M = Fe, Ru, and Os) compounds at low temperatures due to the strong c-f hybridization. However, $CeRu_2Al_{10}$ exhibits qualitatively the same phase transition as $CeOs_2Al_{10}$, whereas $CeFe_2Al_{10}$ has no phase transition.

B. Seebeck coefficient

Seebeck coefficient and thermal conductivity measurements were simultaneously performed in a close-cycle helium refrigerator by the direct heat pulse technique. Further details about the experimental techniques can be found elsewhere.[26,27] Temperature variation of $S(T)$ for $CeOs_2Al_{10}$ is illustrated in Fig. 3. The striking feature in $S(T)$ is the presence of an abrupt drop near T_0, followed by a sharp upturn upon further cooling. These phenomena are strongly related to the phase transition and the characteristic of a narrow band around the Fermi surface. The diffusion part of S in heavy-fermion and Kondo systems is completely dominant over the phonon drag contributions, leading to a broad maximum and minimum at 100 and 10 K, respectively. This signature has been commonly found in many Ce-based compounds such as $CeRu_2Al_{10}$, $CeCu_2Si_2$, and $CeAl_3$.[4,28,29]

In principle, the Seebeck coefficient is proportional to the logarithmic energy derivative of the DOS at the Fermi level. Therefore, within the framework of the two-band scenario as described in the previous section, the contribution to S from the narrow f band is expected to be proportional to $P/(w^2 + P^2)$, and the total measured S is given by the expression

$$S = c_1 T + c_2 T \frac{P}{P^2 + W^2}, \tag{2}$$

where T-independent parameters c_1 and c_2 are relevant to contributions from nonmagnetic and magnetic scattering processes, respectively. For a first glance at Eq. (2), it seems that S is proportional to T. However, considering the fact that the parameters P and W are temperature dependent, the resulting $S(T)$ could be rather complicated. It is indeed the case for the present $CeOs_2Al_{10}$ system where a dome-shaped feature was found in $S(T)$ above the phase transition. The presence of a characteristic maximum (qualitatively $S \sim T$ below the maximum and $S \sim 1/T$ above the maximum) is commonly observed in many compounds with an intermediate

TABLE I. Parameter values corresponding to the fits of the $\rho(T)$ and $S(T)$ data displayed in Figs. 2 and 3 based on the relations in Eqs. (1) and (2) described in the text.

ρ_0 ($\mu\Omega$ cm)	A (K)	B (K)	m (K)	q_f (K)	D ($\mu\Omega$ cm K)	c ($\mu\Omega$ cm K^{-1})	c_1 (μV/K^2)	c_2 (μV/K)
525	7	80	158	30.2	12000	− 0.4528	− 0.37	28.6

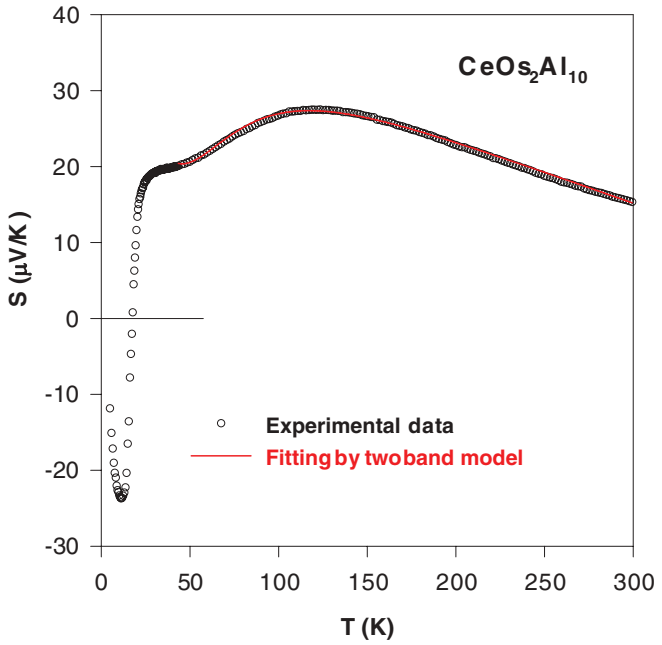

FIG. 3. (Color online) Temperature dependence of Seebeck coefficient $S(T)$ for $CeOs_2Al_{10}$. The solid line is a fit to the experimental data as described by Eq. (2).

valence of Ce due to the crystal-field effect, with which the two-band model could be employed.[30,31] It is evident from Fig. 3, where the solid line is a nonlinear-least-square fit to the experimental data using Eq. (2), that the two-band model describes $S(T)$ quite well over a wide temperature range. The magnitude of $A = 7$ K was determined directly from the slope of the linear portion of $S(T)$ just above T_0, while the constants c_1, c_2, B, m, and q_f were used as free fitting parameters. The parameters A, B, and m extracted from $S(T)$ were employed as fixed values in Eq. (1) for the $\rho(T)$ analysis. Here q_f directly correlates with $\rho(T)$, and the optimum q_f as well as other parameters were obtained by refining both $S(T)$ and $\rho(T)$ iteratively. The yielded $q_f = 30.2$ K corresponding to the quasielastic linewidth $\Gamma_{QE} \sim 2.6$ meV is close to the width (Fig. 6 in Ref. 19) observed from inelastic neutron scattering measurements.[17] The reliable physical parameters revealed from $S(T)$ and $\rho(T)$ data analyses were tabulated in Table I. As mentioned above, $S(T)$ drops rapidly with a sign change from positive to negative around 17 K, where the phase transition involves the development of the unconventional spin-density-wave (SDW) state or the hidden-order state.[32] It is apparent that $S(T)$ exhibits an upturn at around 10.5 K and tends to approach to zero with further decreasing temperature as required thermodynamically. The sign revisal in $S(T)$ implies a change of conduction mechanism or dominant carrier of $CeOs_2Al_{10}$ below 17 K. Such behavior is likely attributed to the sudden change of the band structure associated with the electron-hole asymmetry. A recent μSR study has revealed that the resonance frequency and muon depolarization rate show anomalous features below 18 K,[19] at which a lattice distortion was confirmed by a recent electron-diffraction study.[16] These phenomena are presumably intertwined and certainly warrant further investigations.

From the Seebeck coefficient result, $CeOs_2Al_{10}$ contains light hole pockets in its energy band below the transition, but in the high-temperature regime the holes become heavier and thus dominate the Seebeck coefficient. It is also instructive to compare the thermoelectric behavior between $CeRu_2Al_{10}$ and $CeOs_2Al_{10}$ in the ordered state. For the case of $CeRu_2Al_{10}$,[4] S is originally negative and then changes sign to positive at $\sim$18 K, while $CeOs_2Al_{10}$ exhibits an opposite trend. It appears that the phase transition has the same effect in the Seebeck coefficient for both compounds in the ordered state, showing a peak feature at $\sim$10 K. However, the different sign in S at the lowest measurable temperature indicates that the corresponding Fermi level ε_F for $CeOs_2Al_{10}$ ($CeRu_2Al_{10}$) resides at the rising (falling) portion of the conduction band DOS as that would yield a positive (negative) value of $\partial \ln N(\varepsilon)/\partial\varepsilon$ at ε_F. This is consistent with the high-pressure studies that the corresponding ε_F for $CeRu_2Al_{10}$ and $CeOs_2Al_{10}$ locates at opposite sides of the center of gravity of the $4f$ band. These observations based on Seebeck coefficient measurements would provide experimental information for future band-structure calculations of $CeOs_2Al_{10}$ and related compounds.

C. Thermal conductivity

The total T-dependent thermal conductivity $\kappa(T)$ for $CeOs_2Al_{10}$ is shown in Fig. 4. Upon cooling, $\kappa(T)$ increases smoothly and then develops a broad peak at around 32 K due to the reduced thermal scattering of heat carrying phonons. With further decreasing temperature, $\kappa(T)$ falls slowly with a noticeable minimum at $T_{min} \sim 23$ K. Below T_{min}, $\kappa(T)$ exhibits a sudden enhancement with a peak at around 19 K, close to the temperature where the sign of the Seebeck coefficient changes. In principle, the total thermal conductivity for ordinary metals

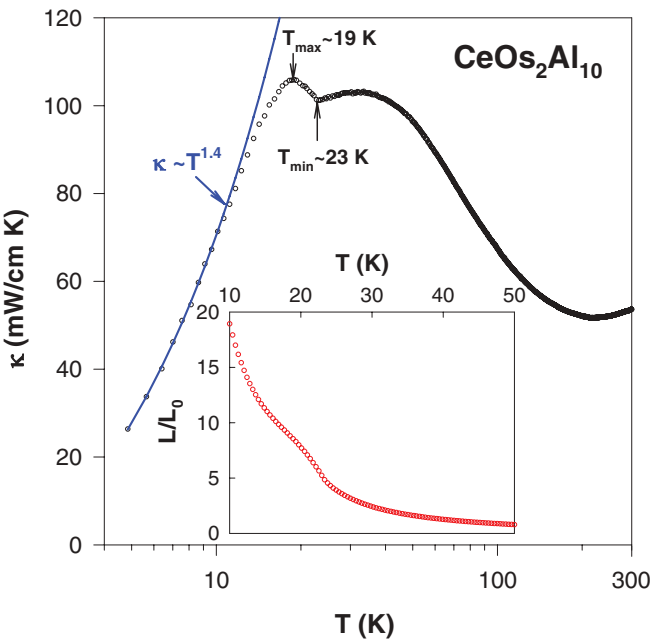

FIG. 4. (Color online) Temperature variation of the total thermal conductivity $\kappa(T)$ for $CeOs_2Al_{10}$. The inset shows the Lorentz number normalized to the Sommerfeld value as a function of temperature.

and semimetals is expressed as a sum of electronic and lattice terms. The electronic thermal conductivity (κ_e) can be evaluated using the Wiedemann-Franz law $\kappa_e \rho/T = L_0$, where ρ is the measured dc electric resistivity and $L_0 = 2.45 \times 10^{-8}$ W Ω K^{-2} is the Lorentz number. This estimate gives a very small contribution of κ_e, suggesting that the thermal conductivity shown in Fig. 4 is essentially due to the lattice thermal conductivity (κ_L). It is quite unusual that a rare-earth compound with ten Al atoms per formula unit has a negligible electronic contribution to the total thermal conductivity. This could be a consequence of the strong hybridization of the localized $4f$ electrons of Ce with conduction electrons that leads to the Kondo insulator behavior in the present case of $CeOs_2Al_{10}$.

The normalized Lorentz number L/L_0 as a function of temperature is displayed in the inset of Fig. 4. Here $L = \kappa\rho/T$ is associated with measured κ and ρ. The decrease of L/L_0 with respect to temperature is a consequence of the strong temperature dependence in the electrical resistivity. However, the observed sudden enhancement in L/L_0 near the phase transition is presumably attributed to the existence of an additional heat transport introduced by ordering. It should be noted that the observed feature resembles that of the isostructural compound $CeRu_2Al_{10}$.[4] Similar observations were also found in other Kondo systems such as URu_2Si_2 (Ref. 6) and CDW systems such as $R_5Ir_4Si_{10}$ and $Lu_5Rh_4Si_{10}$.[33–35]

Now we discuss possible origins of the peak feature around 19 K, which is considerably lower than T_0. It is noted that this signature is in great resemblance to that found in URu_2Si_2 where most of the carriers disappear in the order state, leading to a drastic increase in phononic and electronic mean free paths. It has been justified that the occurrence of the hidden-order results in an excessive enhancement of the thermal conductivity in URu_2Si_2.[6] The peak feature in κ below T_0 also shows that there must be an existence of exotic heat transport introduced by the ordering as that for URu_2Si_2. The possibility of other quasiparticles such as polarons arising from the lattice distortion (or crystal structure modification) during the phase transition or a new phonon excitation spectrum accompanying the phase transition cannot be ruled out with the present stage of the investigation. It is more likely that the observed peak feature around 19 K is due to the magnon-mediated thermal conductivity associated with unconventional magnetic ordering in $CeOs_2Al_{10}$. While the true origin involving the details of magnon-defect, magnon-phonon, and mangon-magnon scattering, the strong anomaly in κ should lie in the peculiar character of the phase transition. It is worthwhile mentioning that a similar feature in κ has been found in the spin-Peierls system NaV_2O_5 which exhibits a huge peak in κ below the phase-transition temperature.[36]

In addition, by the generalized simple kinetic equation, the lattice thermal conductivity is given as $\kappa_L = C_v v l$, where C_v is the phonon specific heat, v represents the phonon drift velocity, and l is the mean free path. The phonon drift velocity and mean free path are expected not to be greatly influenced by the transition. Within the low-temperature limit, κ_L should obey a T^3 dependence based on the Debye model. However, we found a weaker T dependence of $T^{1.4}$ below 10 K for the present case of $CeOs_2Al_{10}$, as indicated by the solid line in Fig. 4. Such a finding suggests that there exists an additional phonon scattering mechanism such as grain boundary that limits the phonon mean free path and hinders the heat flow at low temperatures. It should be noted that the phase transition for this compound is accompanied by a small but finite ordered magnetic moment, as evidenced by the recent neutron diffraction experiments.[19] In such a magnetic ordered state, the magnons may also scatter phonons that are involved in the heat conduction. Another possibility may arise from the unique crystal structure of $CeOs_2Al_{10}$. As mentioned, the Ce atom is surrounded by four Os and 16 Al atoms which form a polyhedron with Ce atoms constructing a zigzag chain along the orthorhombic c axis. At low temperatures, the anharmonic lattice vibration modes in the heat capacity are captured in this oversized cage framework, acting as an effective scattering mechanism for the propagation of heat carrying phonons. As compared to $CeRu_2Al_{10}$ where κ_L follows a T^2 law at low temperature,[1] the relative weak T dependence of $T^{1.4}$ for $CeOs_2Al_{10}$ can be attributed to the fact that Os (~190 amu) is much heavier than Ru (~101 amu). Further investigations are needed to verify these speculations.

D. Specific heat

Specific heat measurement was carried out with a high-resolution ac calorimeter, using chopped light as a heat source. The experimental specific heat C_P result of $CeOs_2Al_{10}$ is given in Fig. 5. The unambiguous evidence for the presence

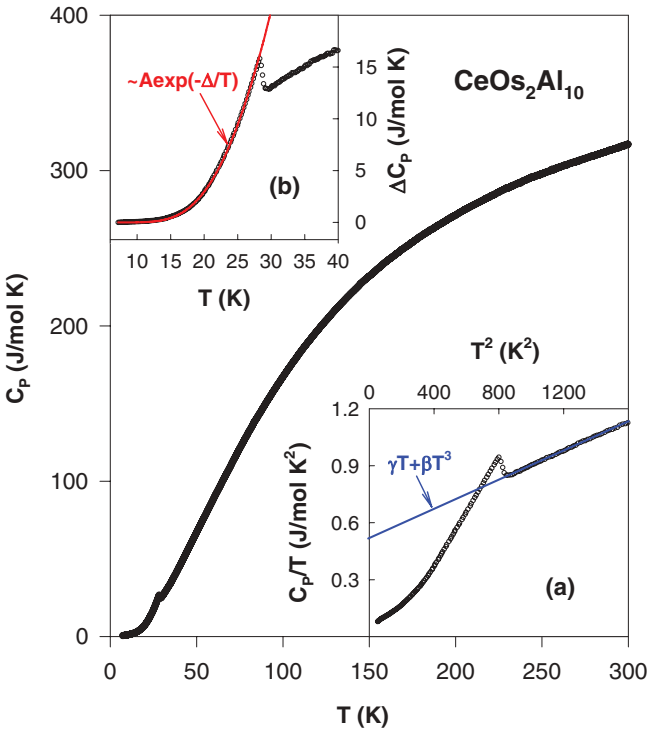

FIG. 5. (Color online) Temperature dependence of the specific heat $C_P(T)$ for $CeOs_2Al_{10}$. Inset (a) shows a C_P/T vs T^2 plot in the vicinity of T_0. A linear fit to the experimental data above T_0 is used to calculate Debye temperature Θ_D and Sommerfield coefficient γ. Inset (b) displays excess specific heat, $\delta C_P(T) \equiv C_P(T) - \gamma T - \beta T^3$ related to the phase transition as a function of temperature. The solid line is the fit to data with an expression $\delta C_P(T) = A_0 \exp(-\Delta_C/T)$.

of a phase transition is associated with a peak feature near 28 K which scarcely changes under the magnetic field up to 14 T, irrespective of the field direction applied to the single crystal of $CeOs_2Al_{10}$.[16] The shape of specific heat jump ΔC_P is reminiscent of a second-order mean-field transition. As shown in the inset (a) of Fig. 5, the specific heat above T_0 obeys $C_P = \gamma T + \beta T^3$, with $\gamma = 514$ mJ/mol K^2 and $\beta = 0.387$ mJ/mol K^4. Since the cubic term is mainly from phonon contributions, we thus obtained the value of the Debye temperature $\Theta_D = 402$ K for $CeOs_2Al_{10}$. The large γ indicates that $CeOs_2Al_{10}$ belongs to the family of heavy-fermion systems and a value of 370 mJ/mol K^2 has also been deduced from a single crystal.[3] In addition, the specific heat jump $\Delta C_P = 3.63$ J/mol K was estimated near T_0.[3]

The excess specific heat $\delta C_P(T) \equiv C_P(T) - \gamma T - \beta T^3$ can be well described by a thermally activated form $\delta C_P(T) = A_0 \exp(-\Delta_C/T)$ with $A_0 = 997$ J/mol K and $\Delta_C = 116$ K $= 4.14 T_0$ [solid line in the inset (b) of Fig. 5]. Hence, the specific heat data clearly reveals that the anomaly associated with a second-order phase transition involves an energy gap of about 116 K (10 meV) over a portion of Fermi surfaces which is a bit larger than its isostructural compound $CeRu_2Al_{10}$.[4] The extracted energy gap is also comparable to the value of 11 meV inferred from the recent inelastic neutron scattering experiment and the NMR results of $CeOs_2Al_{10}$.[19,24]

E. Thermal expansion

The length change and linear thermal expansion were measured over temperatures from 10 to 40 K using a capacitance dilatometer. Figure 6 shows the coefficient of thermal expansion α for $CeOs_2Al_{10}$ in the vicinity of the transition. A clear jump in is seen in response to the onset of second-order phase transition at T_0. It is also noted that the thermal expansion anomaly at ~27 K shares similar features as C_P, suggesting a close thermodynamic relationship for this transition. The T-dependent Gruneisen ratio in terms of α/C_P is illustrated in the inset of Fig. 6. As one can see, the ratio exhibits a weak temperature dependence above T_0 and practically a constant above 40 K. Such an observation suggests a single energy scale and only the phonon degree of freedom is relevant to this temperature range. An anomalous feature is also seen in the Gruneisen ratio, indicating that the electronic and magnetic contributions may come into play at the phase transition.

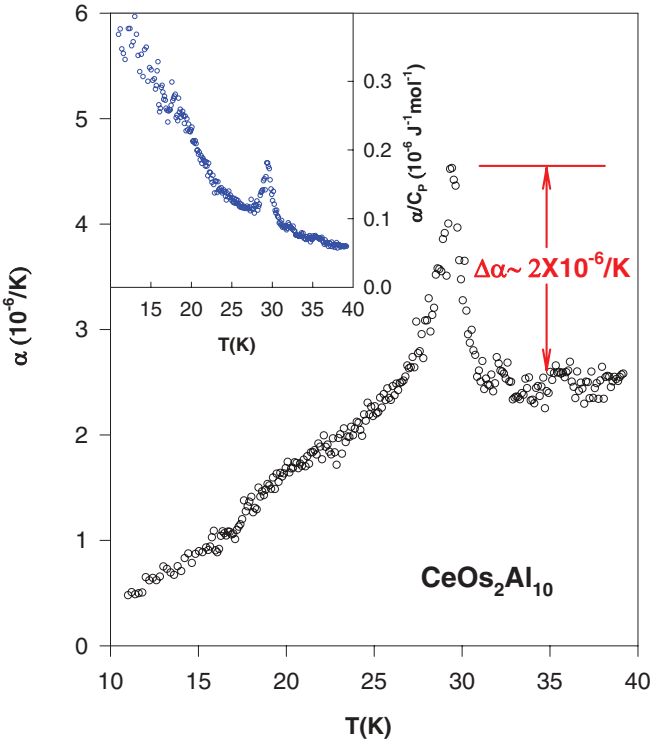

FIG. 6. (Color online) Coefficient of linear thermal expansion $\alpha(T)$ of $CeOs_2Al_{10}$ as a function of temperature. Inset: temperature dependence of Grüneisen ratio α/C_P, for $CeOs_2Al_{10}$.

According to the Ehrenfest relation, the specific heat anomaly can be related to the thermal expansion for a second-order transition as

$$\Delta\alpha = \frac{1}{3V}\left(\frac{\Delta C_P}{T_0}\right)\left(\frac{dT_0}{dP}\right). \quad (3)$$

Substituting the experimental values $\Delta\alpha = +2.1 \times 10^{-6}$ (1/K), $\Delta C_P = 3.6$ (J/mol K), $T_0 = 28$ K, and the molar volume $V = 1.3 \times 10^{-4}$ (m^3/mol) to Eq. (3), it yields $dT_0/dP = +6.32$ (K/GPa) which indicates a rather large enhancement of T_0 under hydrostatic pressure for $CeOs_2Al_{10}$. It is noted that the calculated pressure dependence on the transition temperature of $CeOs_2Al_{10}$ is quite similar to that of $CeRu_2Al_{10}$ with $dT_0/dP = +6.03$(K/GPa), where there should be a slight increase in T_0 at low pressure.[4] Our estimated dT_0/dP agrees very well with the experimental result obtained by Nishioka *et al.* in the case of $CeRu_2Al_{10}$.[5] However, Umeo *et al.* reported a very weak reduction in T_0 at low pressure and then disappears at 2.5 GPa for $CeOs_2Al_{10}$.[37] It is actually very intricate to determine the exact value of T_0 as the appearance of a broad hump has been observed in the pressure-dependent studies.[19] Therefore, we speculate that the discrepancy between our estimated and other reported values is presumably due to the fact that the phase transition is strongly suppressed under pressure, while the precise definition of T_0 is difficult.[5] Another possibility is that the phase transition of $CeOs_2Al_{10}$ disappears at a lower pressure (~2.5 GPa) than that of $CeRu_2Al_{10}$ (~4 GPa), leading to an earlier suppression of T_0 under pressure for $CeOs_2Al_{10}$ as compared to $CeRu_2Al_{10}$.

III. CONCLUSIONS

The Kondo lattice $CeOs_2Al_{10}$ undergoing a mean-field-like second-order phase transition has been established by specific heat and thermal expansion measurements. In the vicinity of the phase transition, all measured physical properties exhibit anomalous features and a concrete estimate of the energy gap $\Delta \sim 116$ K was obtained from the analysis of low-T specific heat. Above the phase transition temperature, the electrical resistivity and Seebeck coefficient can be described by a two-band model with a set of reliable physical parameters. The quasielastic linewidth $q_f \sim 30.2$ K determined from this model is consistent with the value revealed by neutron scattering studies. The peculiar features observed in the Seebeck coefficient and thermal conductivity near the phase

transition, are reminiscent of the hidden-order phase transition for URu_2Si_2. In addition, the peak characteristic found in the thermal conductivity below T_0 enlightens the existence of exotic heat transport introduced by the ordering.

ACKNOWLEDGMENTS

This work was supported by the National Science Council of Taiwan under Grants No. NSC-98-2112-M-006-011-MY3 (C.S.L.) and No. NSC-100-2112-M-259-002-MY3 (Y.K.K.).

*ykkuo@mail.ndhu.edu.tw

[1] A. M. Strydom, Physica B **404**, 2981 (2009).
[2] V. H. Tran, S. Paschen, A. Rabis, N. Senthilkumaran, M. Baenitz, F. Steglich, P. de V. du Plessis, and A. M. Strydom, Phys. Rev. B **67**, 075111 (2003).
[3] M. B. Maple, J. W. Chen, Y. Dalichaouch, T. Kohara, C. Rossel, M. S. Torikachvili, M. W. McElfresh, and J. D. Thompson, Phys. Rev. Lett. **56**, 185 (1986).
[4] C. S. Lue, S. H. Yang, A. C. Abhyankar, Y. D. Hsu, H. T. Hong, and Y. K. Kuo, Phys. Rev. B **82**, 045111 (2010).
[5] T. Nishioka, Y. Kawamura, T. Takesaka, R. Kobayashi, H. Kato, M. Matsumura, K. Kodama, K. Matsubayashi, and Y. Uwatoko, J. Phys. Soc. Jpn. **78**, 123705 (2009).
[6] K. Behnia, R. Bel, Y. Kasahara, Y. Nakajima, H. Jin, H. Aubin, K. Izawa, Y. Matsuda, J. Flouquet, Y. Haga, Y. Onuki, and P. Lejay, Phys. Rev. Lett. **94**, 156405 (2005).
[7] C. S. Garde and J. Ray, J. Phys.: Condens. Matter **6**, 8585 (1994); Phys. Rev. B **51**, 2960 (1995).
[8] S. Murayama, C. Sekine, A. Yokoyanagi, K. Hoshi, and Y. Onuki, Phys. Rev. B **56**, 11092 (1997).
[9] M. Matsumura, Y. Kawamura, S. Edamoto, T. Takesaka, H. Kato, T. Nishioka, Y. Tokunagai, S. Kambe, and H. Yasuokai, J. Phys. Soc. Jpn. **78**, 123713 (2009).
[10] H. Tanida, D. Tanaka, M. Sera, C. Moriyoshi, Y. Kuroiwa, T. Takesaka, T. Nishioka, H. Kato, and M. Matsumura, J. Phys. Soc. Jpn. **79**, 043708 (2010).
[11] S. C. Chen and C. S. Lue, Phys. Rev. B **81**, 075113 (2010).
[12] H. Tanida, D. Tanaka, M. Sera, S. Tanimoto, T. Nishioka, M. Matsumura, M. Ogawa, C. Moriyoshi, Y. Kuroiwa, J. E. Kim, N. Tsuji, and M. Takata, Phys. Rev. B **84**, 115128 (2011).
[13] I. Ishii, Y. Suetomi, H. Muneshige, T. K. Fujita, Y. Muro, J. Kajino, T. Takabatake, and T. Suzuk, J. Phys. Soc. Jpn. **80**, SA045 (2011).
[14] V. M. T. Thiede, T. Ebel, and W. Jeitschko, J. Mater. Chem. **8**, 125 (1998).
[15] A. I. Tursina, S. N. Nesterenko, E. V. Murashova, I. V. Chernyshev, H. Noel, and Y. D. Seropegin, Acta Crystallogr., Sect. E **61**, i12 (2005).
[16] Y. Muro, J. Kajino, K. Umeo, K. Nishimoto, R. Tamura, and T. Takabatake, Phys. Rev. B **81**, 214401 (2010).
[17] Y. Muro, K. Motoya, Y. Saiga, and T. Takabatake, J. Phys. Soc. Jpn. **78**, 083707 (2009).
[18] D. D. Khalyavin, A. D. Hillier, D. T. Adroja, A. M. Strydom, P. Manuel, L. C. Chapon, P. Peratheepan, K. Knight, P. Deen, C. Ritter, Y. Muro, and T. Takabatake, Phys. Rev. B **82**, 100405(R) (2010).
[19] D. T. Adroja, A. D. Hillier, P. P. Deen, A. M. Strydom, Y. Muro, J. Kajino, W. A. Kockelmann, T. Takabatake, V. K. Anand, J. R. Stewart, and J. Taylor, Phys. Rev. B **82**, 104405 (2010).
[20] A. Kondo, J. Wang, K. Kindo, T. Takesaka, Y. Ogane, Y. Kawamura, T. Nishioka, D. Tanaka, H. Tanida, and M. Sera, J. Phys. Soc. Jpn. **80**, 013701 (2011).
[21] K. Hanzawa, J. Phys. Soc. Jpn. **80**, 023707 (2011).
[22] J. Robert, J. M. Mignot, G. André, T. Nishioka, R. Kobayashi, M. Matsumura, H. Tanida, D. Tanaka, and M. Sera, Phys. Rev. B **82**, 100404(R) (2010).
[23] S. I. Kimura, T. Iizuka, H. Miyazaki, A. Irizawa, Y. Muro, and T. Takabatake, Phys. Rev. Lett. **106**, 056404 (2011).
[24] C. S. Lue, S. H. Yang, T. H. Su, and B.-L. Young, Phys. Rev. B **82**, 195129 (2010).
[25] A. Freimuth, J. Magn. Magn. Mater. **68**, 28 (1987).
[26] C. S. Lue and Y. K. Kuo, Phys. Rev. B **66**, 085121 (2002).
[27] C. S. Lue, Y. K. Kuo, S. N. Hong, S. Y. Peng, and C. Cheng, Phys. Rev. B **71**, 064202 (2005).
[28] D. Jaccard, J. M. Mignot, B. Bellarbi, A. Benoit, H. F. Braun, and J. Sierro, J. Magn. Magn. Mater. **47–48**, 23 (1995).
[29] N. B. Brandt and V. V. Moshchalkov, Adv. Phys. **33**, 373 (1984).
[30] M. D. Koterlyn, R. I. Yasnitskii, G. M. Koterlyn, and B. S. Morokhivskii, J. Alloys Compd. **348**, 52 (2003).
[31] D. Kaczorowski and K. Gofryk, Solid State Commun. **138**, 337 (2006).
[32] R. Bel, H. Jin, K. Behnia, J. Flouquet, and P. Lejay, Phys. Rev. B **70**, 220501(R) (2004).
[33] Y.-K. Kuo, C. S. Lue, F. H. Hsu, H. H. Li, and H. D. Yang, Phys. Rev. B **64**, 125124 (2001).
[34] C. S. Lue, Y.-K. Kuo, F. H. Hsu, H. H. Li, H. D. Yang, P. S. Fodor, and L. E. Wenger, Phys. Rev. B **66**, 033101 (2002).
[35] Y.-K. Kuo, F. H. Hsu, H. H. Li, H. L. Huang, C. W. Huang, C. S. Lue, and H. D. Yang, Phys. Rev. B **67**, 195101 (2003).
[36] A. N. Vasil'ev, V. V. Pryadun, D. I. Khomskii, G. Dhalenne, A. Revcolevschi, M. Isobe, and Y. Ueda, Phys. Rev. Lett. **81**, 1949 (1998).
[37] K. Umeo, T. Ohsuka, Y. Muro, J. Kajino, and T. Takabatake, J. Phys. Soc. Jpn. **80**, 064709 (2011).